

Stabilized Femtosecond Lasers for Precision Frequency Metrology and Ultrafast Science

R. J. Jones*, T. Ido, T. Loftus, M. Boyd, A. Ludlow, K. Holman,
M. Thorpe, K. Moll, and J. Ye**

JILA, NIST, and the University of Colorado, 440 UCB Boulder, CO 80309, USA

*e-mail: rjjones@jilau1.colorado.edu

**e-mail: Ye@jila.colorado.edu

Received December 27, 2004

Abstract—We present results from several experiments in which the repetitive, coherent nature of stabilized mode-locked pulse trains are utilized. From absolute optical frequency measurements in ultracold Sr atoms to the coherent storage and amplification of optical pulse trains in high-finesse Fabry–Perot cavities, the stabilized femtosecond laser has become an indispensable tool in precision spectroscopy and ultrafast science.

Stabilization of the carrier-envelope offset phase of optical pulses has opened up new avenues of research in optical frequency metrology and ultrafast science. The same tools used to create a single phase-coherent link between the optical and microwave regimes utilizing the femtosecond (fs) comb [1] have also provided unprecedented control over the temporal properties of the pulse. We discuss our work on the stabilization of fs lasers and new areas of research enabled by this capability. In particular, progress towards an all-optical atomic clock based on the fs laser and narrow transitions in laser-cooled strontium will be reviewed. In addition to precision frequency metrology, the fs laser can be utilized to make accurate measurements of the dispersive properties of “fs enhancement cavities.” Such passive, zero-dispersion cavities are used to coherently build up pulse energy for novel nonlinear intracavity experiments. As an example, we show how the stored intracavity fs pulse can be periodically switched out of the cavity to provide for significant pulse amplification. A net energy gain of 42 to more than 70 times for 38–58-fs pulse durations is demonstrated. Starting with a standard mode-locked laser system, pulses of over 200 nJ are obtained.

The stabilized fs laser can provide the clockwork to reliably link stable optical transitions to the easily countable microwave regime. Current experiments in this area are focused on utilizing narrow intercombination lines in laser-cooled atomic ^{88}Sr . High-resolution spectroscopy of these transitions combined with the precision measurement capability of the fs comb allows for careful investigation of systematic frequency shifts (caused by probing/trapping fields) or other instabilities. For example, Fig. 1 shows the linewidth achieved between a cw diode laser, used as both a cooling and stable probe beam for the narrow $^1S_0 \rightarrow ^3P_1$ transition in ^{88}Sr , and a single component of the fs comb at 689 nm stabilized directly to a high-finesse reference cavity [2].

Recently, we have used this system to perform the most accurate measurement to date of the $^{88}\text{Sr } ^1S_0\text{--}^3P_1$ optical clock transition frequency and to observe, for the first time, definitive density-related line center shifts and spectral broadening of an optical clock transition in ultracold atoms [3]. Figure 2a depicts the ultracold ^{88}Sr spectrometer, while Fig. 2b gives a simplified ^{88}Sr energy-level diagram. For the measurements described here, ^{88}Sr atoms are first cooled to $\sim 1 \mu\text{K}$ in a $^1S_0\text{--}^3P_1$ magneto-optical trap (MOT) [4, 5] and then released into free space. Subsequently, the atomic cloud is illuminated by two weak, counterpropagating probe beams that selectively excite the $^1S_0 (m=0)\text{--}^3P_1 (m=0)$ transition. The atomic density during spectroscopic probing is varied by changing either the trapped atom number (10^6 to 10^8) or the free-flight time (5 ms to 20 ms) after the atoms are released into free space. The probe beam absolute frequency is continuously measured by a fs optical comb that is locked to a Cs-referenced

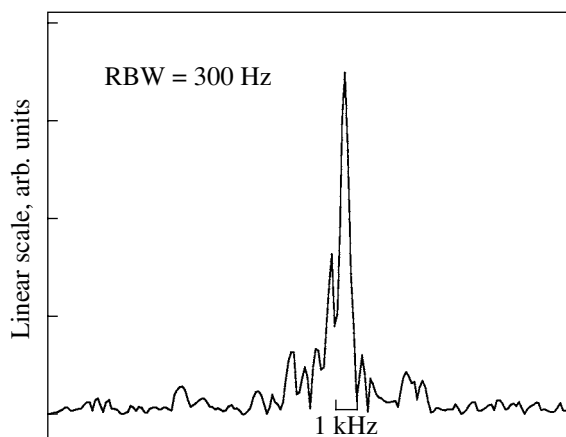


Fig. 1. Beat note (linewidth ~ 300 Hz) between Sr cooling/probe laser and a single component of the fs comb. RBW is resolution bandwidth.

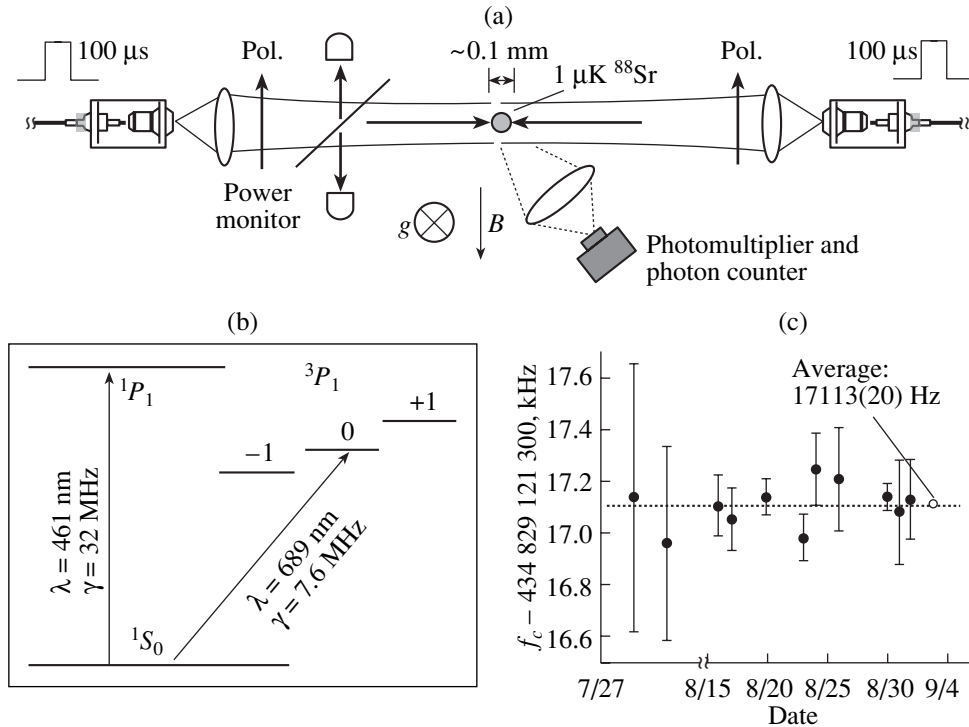


Fig. 2. (a) Top view of the ultracold ^{88}Sr spectrometer. The two counterpropagating beams are first collimated and then overlapped by back-coupling each beam into the opposing fiber launcher. The beam intensities are balanced to within 2.5% via atomic fluorescence signals. Light polarization is parallel to the 4.6(2)-G bias magnetic field. (b) Simplified ^{88}Sr level diagram. γ is the transition linewidth. (c) Accumulated record of the 1S_0 - 3P_1 optical clock transition frequency. Each entry is the weighted average of several independent measurements and is referenced to the NIST Cs fountain clock.

hydrogen maser via a fiber optic link to NIST [6]. By performing absolute frequency measurements for atomic densities spanning three orders of magnitude, from 10^9 to 10^{12} cm^{-3} , we find the linear shift and homogeneous broadening coefficients of $-1.3(3) \times 10^{-9}$ Hz/cm^3 and $2.8(3) \times 10^{-8}$ Hz/cm^3 , respectively. Figure 2c shows absolute measurements of the 1S_0 - 3P_1 line center optical frequency f_c accumulated over two months. Each entry is the weighted average of multiple independent measurements. A majority of the measurements are performed in the low-density regime, and each is corrected for the density shift described above. The final weighted mean is 434829121317113 Hz, with a statistical uncertainty of 20 Hz. From a detailed analysis of systematic frequency shifts and their uncertainties, the systematic correction to the measured frequency is $-4779(33)$ Hz, where the correction (correction uncertainty) is dominated by the single-photon recoil frequency (2.5% probe beam intensity balance). Applying this correction, the 1S_0 - 3P_1 transition frequency is $434829121312334 \pm 20_{\text{stat}} \pm 33_{\text{sys}}$ Hz. This level of measurement precision surpasses recent studies performed with a thermal atomic beam by more than a factor of 200 [7].

The control and stabilization of fs pulse trains enables measurements beyond optical frequency

metrology. For example, many applications in ultrafast science require higher pulse energies than are typically available from standard femtosecond laser oscillators. The ability to stabilize and precisely control an ultrashort pulse train allows for the coherent coupling and enhancement of ultrashort pulses in external high-finesse optical cavities. A passive optical cavity can be used to coherently superpose and temporarily store sequential pulses from a mode-locked laser. The resulting intracavity pulse can be used for the stabilization of femtosecond lasers [8], nonlinear frequency conversion [9], intracavity spectroscopy [10], and coherent pulse “amplification” [11, 12] when the cavity is equipped with a Bragg cell for pulse picking (see Fig. 3). This approach leads to an effective amplification process through decimation of the original pulse rate while preserving the original CE phase coherence from the oscillator. Unlike in actively damped laser systems, the pulse energy is not limited by the saturation of a gain medium or saturable absorber. Instead, the pulse energy can continue to build up inside the passive storage cavity until it is limited by scattering loss and dispersion. The use of a passive cavity also enables amplification of short pulses where no suitable active gain medium may exist, such as in pulse trains generated in the infrared from difference-frequency mixing [13] or in the UV from harmonic generation. In our previous work, we

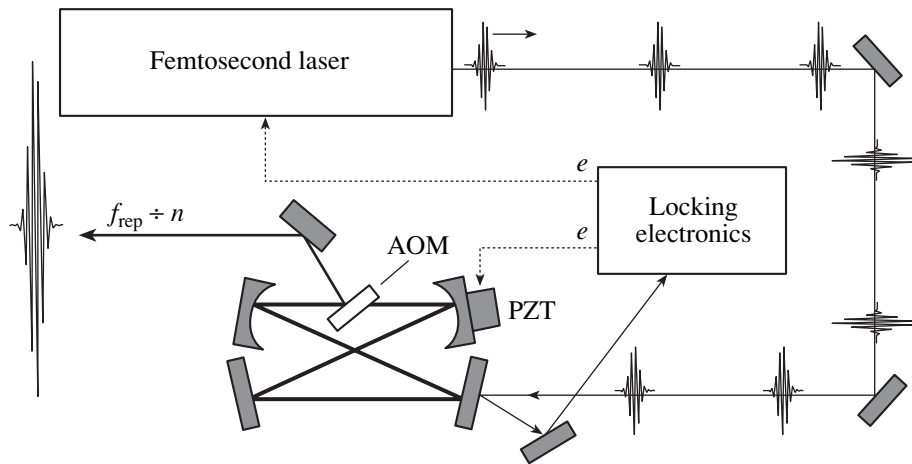


Fig. 3. Simplified schematic of pulse amplification with a fs enhancement cavity. Coherent accumulation and subsequent dumping of the passive cavity results in amplified pulse energies at repetition rates reduced n -fold.

demonstrated this principal of coherent amplification with picosecond pulses [12] in which the role of cavity dispersion and the effects of the carrier-envelope offset frequency (f_{ceo}) were negligible. We report the extension of this technique into the sub-50-femtosecond regime and demonstrate results for “noise-free” amplification of fs pulses by coherently storing and periodically dumping broadband pulses inside a high-finesse, passive optical cavity.

Figure 3 shows a schematic for the enhancement of fs pulses. The pulse train is first mode-matched to the fs enhancement cavity, with the cavity length matching that of the spacing between incident pulses. Error signals are obtained by detecting the reflected light and subsequently used to lock the two degrees of freedom of the fs laser to the enhancement cavity [2]. The first error signal (e_1) is sent to the enhancement cavity to keep the phase and frequency of the stored pulse resonant with the incident pulse train. The second error signal (e_2) is used to lock the laser repetition rate to the cavity. With both locks activated, the intracavity power coherently builds up until it either reaches its steady-state value or is switched out by the AOM. This periodic cavity dumping results in an overall reduction in the repetition rate by n times and provides a single-pulse energy gain G .

The maximum bandwidth (i.e., the shortest pulse) that can be coupled into the cavity is limited by the net group delay dispersion (GDD) of the cavity, as discussed in [11]. The higher the cavity finesse, the more severe the effects of nonzero GDD due to the longer lifetime of the pulse inside the cavity. To compensate for the dispersion of the 3.8 mm of fused silica from the intracavity AOM, negative GDD mirrors based on a double Gires–Tournois interferometer design [14] were used in the cavity. Three bounces per round trip from these mirrors provided -120 fs^2 of GDD compensation. Fine tuning of the cavity dispersion was accomplished by adjusting the air pressure of the chamber containing

the fs enhancement cavity. This provided $\approx 60 \text{ fs}^2$ of tunability when changing from atmospheric pressure to $<1 \text{ Torr}$ and was crucial to the coupling of the shortest pulses into the cavity.

As with the ps enhancement cavity, the overall gain depends on intracavity losses, impedance and mode matching, the dumping efficiency of the intracavity AOM, and the pulse dumping rate for a given cavity finesse. Faster switching times easily allow for the generation of pulse trains of over 1 MHz at the expense of decreased gain but are not optimum with our cavity design due to the $>1\text{-}\mu\text{s}$ cavity lifetime. With fs pulses, a decreased gain also accompanies shorter pulses as a consequence of the less restrictive spectral filtering by the cavity. With a 0.9% input coupler at 800 nm and a pulse dumping efficiency of $\sim 40\%$, the overall gain obtained with the fs enhancement cavity varied from $42\times$ with 39-fs pulses to over $70\times$ with 52-fs pulses for dumping rates below 500 kHz. Greater pulse enhancements are still possible with reduced intracavity losses (currently $<0.5\%$) and improved impedance matching.

Measurements of fs pulse enhancement for this range are shown in Fig 4. A $\sim 200\text{-kHz}$ pulse train was generated from the 100-MHz laser. The input (output) spectrum for two pulse trains with different spectral bandwidths is indicated by the dotted (solid) curves in panels (a) and (b) of Fig. 4. The pulse was stretched (compressed) with a grating-based system before (after) the enhancement cavity to minimize the intracavity nonlinear response. The efficiency of the stretcher and compressor was only $\approx 45\%$ each. The recompressed pulse switched out of the cavity was measured with a frequency-resolved optical gating (FROG)-based system (Figs. 4c and 4d show the measured pulses corresponding to the spectra of Figs. 4a and 4b, respectively). With the pulses stretched to over 100 ps, the limitation on the energy achieved per pulse was due to the inefficiency of the gratings and the limited power available from the Ti:sapphire laser. For Figs. 4b and

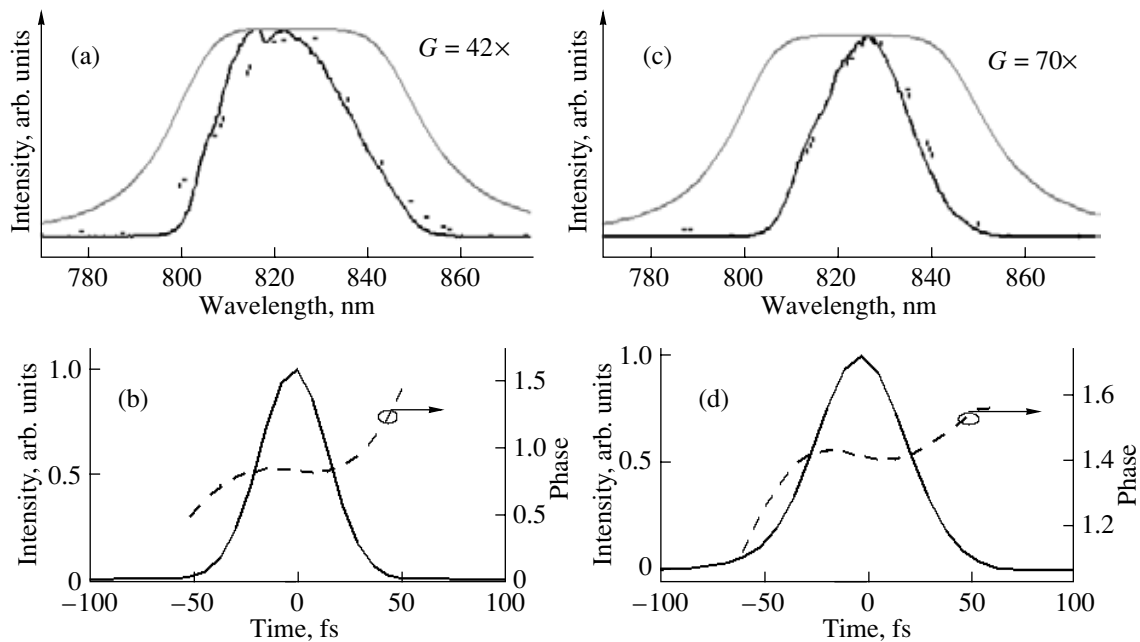


Fig. 4. Pulse spectrum and recompressed pulse intensity and phase measured by FROG after cavity enhancement. (a) and (c) show the incident (dotted) and intracavity (solid) pulse spectrum for two different incident pulse bandwidths. The solid gray line indicates the calculated spectral transfer function based on the third-order dispersion of the intracavity fused silica. (b) and (d) show the corresponding pulse measurements of 39-fs and 52-fs pulses (FWHM), respectively.

4d, the incident pulse energy of 2.5 nJ was increased $70\times$ to 175 nJ before recompression. When the laser was adjusted to produce 58-fs pulses, the incident pulse energy available went up to 3 nJ, resulting in enhanced pulse energies of 210 nJ from the cavity before recompression back to 58 fs. A prism-based stretcher-compressor system [15] would provide a much greater throughput and will make more efficient use of the power available from the laser, enabling pulse energies greater than 400 nJ to be generated starting with only conventional oscillators.

The current limitation on the efficient enhancement of shorter pulses is consistent with that expected from the TOD of the AOM, given our current cavity finesse. Numerical calculations taking only the TOD of the intracavity fused silica into account and assuming an incident spectrum as shown in Fig. 4a predict an intracavity bandwidth supporting an ≈ 38 -fs FTL pulse duration, similar to that actually measured in Fig 4c. This calculated spectral transfer function is shown as the thick grey line in Figs. 4a and 4c. These measurements indicate that it will be possible to enhance sub-30-fs pulses by comparable amounts when TOD is taken into account in the overall cavity design.

In conclusion, we have shown examples of the impact that stabilized fs lasers have had in such disparate fields as optical frequency metrology and ultrafast science. The phase-coherent relationship between the repetition rate of the fs laser and the optical frequencies of its comblike structure enable precision measurements of absolute optical frequencies. Likewise, the ability to stabilize and control these frequencies enables

the manipulation of the pulsed light field and allows, among other possibilities, the coherent addition and storage of ultrashort light pulses inside high-finesse cavities. Such enhancement cavities will allow the use of stabilized, high-repetition-rate pulse trains directly from the oscillator to study nonlinear phenomena previously restricted to low-repetition, actively amplified systems.

REFERENCES

1. D. J. Jones *et al.*, *Science* **288**, 635 (2000).
2. R. J. Jones, I. Thomann, and J. Ye, *Phys. Rev. A* **69**, 051803(R) (2004).
3. T. Ido *et al.*, *Phys. Rev. Lett.* **94**, 153001 (2005).
4. T. H. Loftus *et al.*, *Phys. Rev. Lett.* **93**, 073003 (2004).
5. T. H. Loftus *et al.*, *Phys. Rev. A* **70**, 063413 (2004).
6. J. Ye *et al.*, *J. Opt. Soc. Am. B* **20**, 1459 (2003).
7. G. Ferrari *et al.*, *Phys. Rev. Lett.* **91**, 243002 (2003).
8. R. J. Jones and J.-C. Diels, *Phys. Rev. Lett.* **86**, 3288 (2001).
9. G. T. Maker and A. I. Ferguson, *App. Phys. Lett.* **55**, 1158–1160 (1989).
10. T. Gherman and D. Romanini, *Opt. Express* **10**, 1033 (2002).
11. R. J. Jones and J. Ye, *Opt. Lett.* **27**, 1848 (2002).
12. E. Potma, C. Evans, X. S. Xie, *et al.*, *Opt. Lett.* **28**, 1835 (2003).
13. S. Foreman, D. J. Jones, and J. Ye, *Opt. Lett.* **28**, 370 (2003).
14. B. Golubovic, R. R. Austin, M. K. Steiner-Shepard, *et al.*, *Opt. Lett.* **25**, 275 (2000).
15. Z. Cheng, F. Krausz, and C. Spielmann, *Opt. Comm.* **201**, 145 (2002).